177917: metamorphosed tuffaceous sandstone, Round Hill

Location and sampling

WIDGIEMOOLTHA (SH51-14), ERAYINIA (3435)
MGA Zone 51, 452394E 6547059N

Sampled on 4 May 2004

The sample was taken from a 0.5 m diameter boulder at the top of a small rocky ridge on the southwestern shore of an ephemeral lake, about 10 km northeast of Round Hill.

Tectonic unit/relations

The unit sampled is a grey, medium- to fine-grained, recrystallized and metamorphosed tuffaceous sandstone with biotite- and amphibole-rich lenses (Jones, in prep). This sandstone is part of the Mount Belches Formation, within the Bulong Domain of the Kurnalpi Terrane, within the southern Eastern Goldfields Superterrane of the Yilgarn Craton (Cassidy et al., 2006), and is interpreted to be in fault contact with older mafic and ultramafic rocks of the Kurnalpi Terrane to the east (Jones, in prep). To the west, on MOUNT BELCHES, the Mount Belches Formation is intruded by the Kiaki Monzogranite (Painter and Groenewald, 2001).

Petrographic description

The visually estimated primary mineralogy of this sample includes about 55% grains greater than 1 mm in diameter (10–15% quartz, 25% plagioclase, 10% amphibole, and 7–8% biotite), and about 45% recrystallized matrix grains less than 0.3 mm diameter (20% quartz and 25% plagioclase). Coarse-grained quartz and plagioclase form disseminated rounded or elliptical single-crystal grains of detrital origin. Rare lithic clasts, up to 4 mm long, are dominated by quartz and feldspar, with minor biotite, apatite, and opaque oxide minerals, and may represent fragments of felsic volcanic rock. Poorly defined layers and lenses composed variously of biotite and pale-green amphibole (tremolite–actinolite) are abundant but not entirely parallel, and individual crystals are typically non-oriented. Accessory opaque oxides, leucoxene, apatite, rare tourmaline, and rare sulfide are disseminated. Sparse minute radioactive grains form pleochroic haloes in biotite.

Some large plagioclase grains (and some biotite) have been altered to clay minerals. Fractures are filled with prehnite, which also occurs as cleavage-parallel lamellae in biotite. The primary mineralogy of this sample is consistent with upper greenschist or lower amphibolite facies metamorphism of a tuffaceous sandstone, with subsequent retrogression and hydrothermal alteration forming clay minerals and prehnite.

Zircon morphology

Zircons isolated from this sample range from euhedral to anhedral and well-rounded, and are mainly clear and colourless. They are up to 200 µm long and equant to weakly elongate, with aspect ratios between 1:1 and 3:1. Concentric growth zoning is ubiquitous, although in some cases the zoning is disrupted, indicating alteration. Many zircons are pervasively cracked. A cathodoluminescence image of representative zircons is shown in Figure 1.

Analytical details

This sample was analysed on 25 October 2004, using SHRIMP-B. Fifteen analyses of the CZ3 standard were obtained during the session, and indicated a $^{238}U/^{206}Pb^*$ calibration uncertainty of 2.10% (1σ). Common-Pb corrections were applied using Broken Hill common-Pb isotopic compositions for all analyses except 10 (2.1, 17.1, 19.2, 20.1, 21.1, 22.1, 24.1, 31.1, 35.1, and 53.1), which used compositions determined using the method of Stacey and Kramers (1975).

Results

Sixty-one analyses were obtained from 55 zircons, with six grains (16, 19, 26, 27, 31, and 40) each analysed twice. Results are listed in Table 1, and shown in a concordia diagram in Figure 2 and a probability density diagram in Figure 3.

Interpretation

The analyses are concordant to moderately discordant, and the discordance pattern is consistent with both ancient and recent loss of radiogenic Pb from some of the analysed sites. Seven analyses (2.1, 14.1, 17.1, 19.2, 31.1, 37.1, and 53.1) are characterized by high common-Pb contents ($f204$ >1%) or moderate to strong discordance (>10%). Their $^{207}Pb^*/^{206}Pb^*$ dates are imprecise or unreliable, and are not considered geologically significant. The remaining 54 analyses can be divided into three groups based on their $^{207}Pb^*/^{206}Pb^*$ ratios, common-Pb contents, and discordance values.

Group 1 comprises nine slightly discordant analyses of nine zircons (1.1, 16.2, 20.1, 21.1, 24.1, 33.1, 35.1, 40.2, and 48.1) with slightly elevated common-Pb contents ($f204$ >0.2%), and $^{207}Pb^*/^{206}Pb^*$ dates of 2642–2539 Ma.

Group 2 comprises 27 concordant to slightly discordant analyses of 27 zircons (3.1, 4.1, 5.1, 6.1, 11.1, 13.1, 16.1, 18.1, 23.1, 26.1, 27.1, 28.1, 36.1, 38.1, 39.1, 40.1, 41.1, 42.1, 43.1, 44.1, 46.1, 47.1, 49.1, 50.1, 51.1, 54.1,

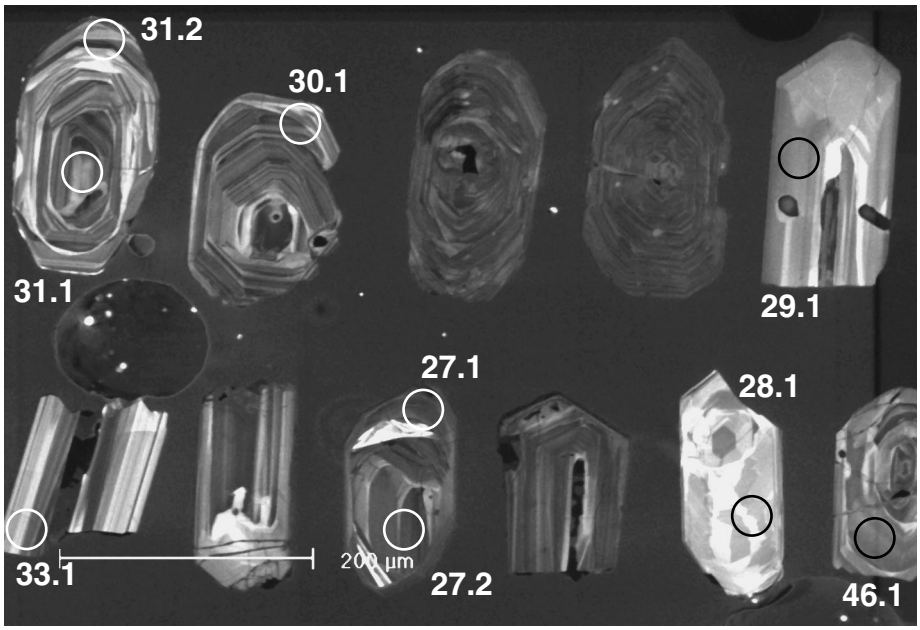

Figure 1. **Cathodoluminescence image of representative zircons from sample 177917: metamorphosed tuffaceous sandstone, Round Hill. Numbered circles represent approximate positions of analysis sites**

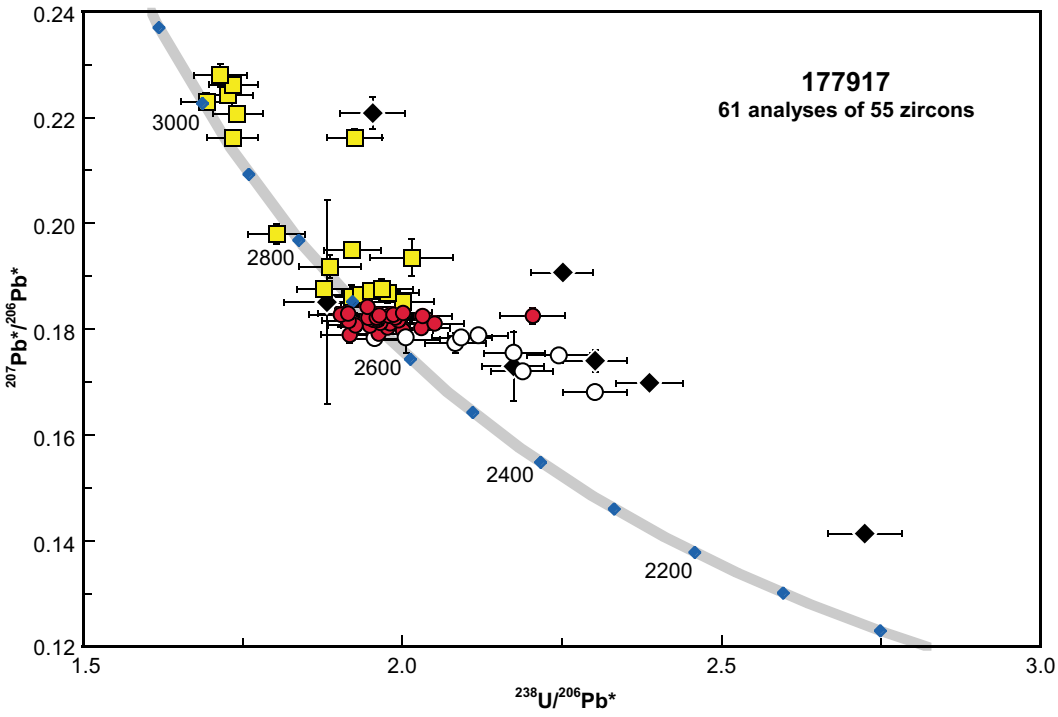

Figure 2. **U–Pb analytical data for sample 177917: metamorphosed tuffaceous sandstone, Round Hill. Open circles denote Group 1 (affected by radiogenic Pb loss during metamorphism); filled circles denote Group 2 (youngest detrital age component); squares denote Group 3 (older detrital zircons); filled diamonds denote ungrouped analyses (discordance >10% or f204 >1%)**

Table 1. Ion microprobe analytical results for zircons from sample 177917: metamorphosed tuffaceous sandstone, Round Hill

Grain .spot	*U (ppm)*	*Th (ppm)*	*Th/U*	*f204 (%)*	$^{238}U/^{206}Pb$ ±1σ	$^{207}Pb/^{206}Pb$ ±1σ	$^{238}U/^{206}Pb^*$ ±1σ	$^{207}Pb^*/^{206}Pb^*$ ±1σ	$^{238}U/^{206}Pb^*$ *age (Ma)* ±1σ	$^{207}Pb^*/^{206}Pb^*$ *age (Ma)* ±1σ	*Disc (%)*
1.1	230	192	0.86	0.143	1.954 ± 0.043	0.17928 ± 0.00092	1.957 ± 0.043	0.17816 ± 0.00101	2661 ± 48	2636 ± 9	–0.9
2.1	314	197	0.65	1.456	2.143 ± 0.047	0.18601 ± 0.00458	2.174 ± 0.049	0.17302 ± 0.00652	2439 ± 45	2587 ± 63	5.7
3.1	227	136	0.62	0.034	1.926 ± 0.042	0.18101 ± 0.00094	1.927 ± 0.043	0.18074 ± 0.00094	2695 ± 49	2660 ± 9	–1.3
4.1	222	226	1.05	0.067	1.915 ± 0.042	0.18212 ± 0.00094	1.916 ± 0.042	0.18159 ± 0.00099	2707 ± 49	2667 ± 9	–1.5
5.1	57	30	0.54	0.127	1.913 ± 0.048	0.18395 ± 0.00189	1.915 ± 0.048	0.18297 ± 0.00202	2708 ± 55	2680 ± 18	–1.0
6.1	103	86	0.86	0.115	1.916 ± 0.045	0.17982 ± 0.00140	1.918 ± 0.045	0.17892 ± 0.00149	2705 ± 52	2643 ± 14	–2.3
7.1	55	32	0.60	0.221	1.917 ± 0.048	0.18793 ± 0.00193	1.921 ± 0.048	0.18621 ± 0.00206	2702 ± 55	2709 ± 18	0.3
8.1	180	53	0.30	0.023	1.877 ± 0.042	0.18775 ± 0.00108	1.877 ± 0.042	0.18757 ± 0.00111	2753 ± 50	2721 ± 10	–1.2
9.1	48	26	0.56	–0.066	1.888 ± 0.048	0.19130 ± 0.00211	1.887 ± 0.048	0.19181 ± 0.00222	2741 ± 57	2758 ± 19	0.6
10.1	68	22	0.33	0.035	1.977 ± 0.049	0.18716 ± 0.00191	1.977 ± 0.049	0.18689 ± 0.00195	2638 ± 53	2715 ± 17	2.8
11.1	150	64	0.44	0.117	1.947 ± 0.044	0.18159 ± 0.00212	1.950 ± 0.044	0.18068 ± 0.00213	2669 ± 50	2659 ± 20	–0.4
12.1	79	71	0.93	0.037	2.001 ± 0.048	0.18547 ± 0.00162	2.002 ± 0.048	0.18518 ± 0.00163	2612 ± 52	2700 ± 15	3.2
13.1	175	137	0.81	0.058	1.954 ± 0.044	0.18226 ± 0.00114	1.955 ± 0.044	0.18180 ± 0.00118	2663 ± 49	2669 ± 11	0.2
14.1	604	14	0.02	0.046	2.249 ± 0.049	0.19105 ± 0.00064	2.250 ± 0.049	0.19069 ± 0.00065	2370 ± 43	2748 ± 6	13.8
15.1	102	62	0.63	0.062	1.935 ± 0.046	0.18698 ± 0.00144	1.936 ± 0.046	0.18650 ± 0.00147	2684 ± 52	2712 ± 13	1.0
16.1	216	247	1.18	0.068	1.985 ± 0.044	0.18327 ± 0.00098	1.987 ± 0.044	0.18274 ± 0.00101	2628 ± 48	2678 ± 9	1.8
16.2	251	216	0.89	0.204	2.115 ± 0.047	0.18039 ± 0.00093	2.119 ± 0.047	0.17880 ± 0.00102	2492 ± 46	2642 ± 10	5.7
17.1	1730	2158	1.29	0.062	2.723 ± 0.058	0.14197 ± 0.00097	2.725 ± 0.058	0.14143 ± 0.00098	2015 ± 37	2245 ± 12	10.2
18.1	61	31	0.53	0.120	1.945 ± 0.049	0.18309 ± 0.00181	1.947 ± 0.049	0.18215 ± 0.00206	2672 ± 55	2673 ± 19	0.0
19.1	113	11	0.10	–0.038	1.923 ± 0.045	0.19465 ± 0.00139	1.922 ± 0.045	0.19494 ± 0.00140	2701 ± 51	2784 ± 12	3.0
19.2	27	10	0.37	17.923	1.545 ± 0.045	0.34440 ± 0.00372	1.883 ± 0.067	0.18517 ± 0.01927	2746 ± 80	2700 ± 172	–1.7
20.1	334	274	0.85	0.698	2.286 ± 0.050	0.17437 ± 0.00082	2.302 ± 0.050	0.16815 ± 0.00118	2326 ± 43	2539 ± 12	8.4
21.1	124	75	0.62	0.863	2.066 ± 0.048	0.18507 ± 0.00130	2.083 ± 0.048	0.17738 ± 0.00184	2527 ± 48	2629 ± 17	3.9
22.1	161	91	0.58	0.400	1.918 ± 0.043	0.21980 ± 0.00124	1.926 ± 0.044	0.21625 ± 0.00158	2696 ± 50	2953 ± 12	8.7
23.1	85	75	0.91	0.053	1.963 ± 0.048	0.17959 ± 0.00158	1.964 ± 0.048	0.17917 ± 0.00160	2653 ± 53	2645 ± 15	–0.3
24.1	424	135	0.33	0.186	2.172 ± 0.047	0.17715 ± 0.00089	2.176 ± 0.047	0.17550 ± 0.00098	2437 ± 44	2611 ± 9	6.6
25.1	71	68	0.98	–0.112	1.970 ± 0.049	0.18669 ± 0.00181	1.968 ± 0.049	0.18755 ± 0.00193	2649 ± 54	2721 ± 17	2.7
26.1	128	42	0.34	0.202	2.200 ± 0.051	0.18410 ± 0.00133	2.205 ± 0.051	0.18253 ± 0.00149	2411 ± 46	2676 ± 14	9.9
26.2	172	96	0.58	0.039	1.742 ± 0.039	0.22102 ± 0.00117	1.742 ± 0.039	0.22073 ± 0.00120	2924 ± 53	2986 ± 9	2.1
27.1	247	23	0.09	0.122	2.049 ± 0.045	0.18203 ± 0.00090	2.051 ± 0.045	0.18108 ± 0.00097	2560 ± 47	2663 ± 9	3.9
27.2	139	139	1.03	0.351	1.729 ± 0.040	0.21887 ± 0.00131	1.735 ± 0.040	0.21625 ± 0.00145	2934 ± 54	2953 ± 11	0.6
28.1	50	51	1.05	0.102	1.902 ± 0.050	0.18355 ± 0.00205	1.904 ± 0.050	0.18275 ± 0.00228	2721 ± 58	2678 ± 21	–1.6
29.1	73	42	0.59	0.193	1.800 ± 0.044	0.19948 ± 0.00175	1.803 ± 0.044	0.19801 ± 0.00191	2844 ± 57	2810 ± 16	–1.2
30.1	98	42	0.45	0.082	1.693 ± 0.040	0.22359 ± 0.00156	1.694 ± 0.040	0.22298 ± 0.00163	2991 ± 57	3002 ± 12	0.4
31.1	64	33	0.54	1.631	1.922 ± 0.050	0.23529 ± 0.00201	1.954 ± 0.051	0.22083 ± 0.00305	2664 ± 57	2987 ± 22	10.8
31.2	147	106	0.75	0.118	1.725 ± 0.039	0.22515 ± 0.00129	1.727 ± 0.039	0.22428 ± 0.00135	2945 ± 54	3012 ± 10	2.2
32.1	75	24	0.33	0.618	1.705 ± 0.042	0.23252 ± 0.00180	1.715 ± 0.042	0.22799 ± 0.00212	2961 ± 58	3038 ± 15	2.5
33.1	52	44	0.87	0.640	1.994 ± 0.052	0.18302 ± 0.00204	2.007 ± 0.052	0.17801 ± 0.00254	2607 ± 56	2634 ± 24	1.0
34.1	124	1020	8.53	0.122	1.949 ± 0.045	0.18813 ± 0.00135	1.952 ± 0.045	0.18719 ± 0.00135	2667 ± 51	2718 ± 12	1.9
35.1	255	126	0.51	0.321	2.087 ± 0.046	0.18124 ± 0.00093	2.094 ± 0.046	0.17838 ± 0.00108	2517 ± 46	2638 ± 10	4.6
36.1	74	68	0.94	0.101	1.987 ± 0.049	0.18298 ± 0.00172	1.989 ± 0.049	0.18219 ± 0.00175	2625 ± 53	2673 ± 16	1.8
37.1	284	200	0.73	0.052	2.386 ± 0.053	0.17025 ± 0.00091	2.387 ± 0.053	0.16983 ± 0.00093	2255 ± 42	2556 ± 9	11.8
38.1	179	134	0.78	0.160	2.027 ± 0.046	0.18149 ± 0.00108	2.030 ± 0.046	0.18024 ± 0.00119	2582 ± 48	2655 ± 11	2.8
39.1	74	23	0.32	0.058	1.959 ± 0.048	0.18244 ± 0.00168	1.960 ± 0.048	0.18199 ± 0.00189	2658 ± 54	2671 ± 17	0.5

Table 1. (continued)

Grain .spot	*U (ppm)*	*Th (ppm)*	*Th/U*	*f204 (%)*	$^{238}U/^{206}Pb$ ±1σ	$^{207}Pb/^{206}Pb$ ±1σ	$^{238}U/^{206}Pb^*$ ±1σ	$^{207}Pb^*/^{206}Pb^*$ ±1σ	$^{238}U/^{206}Pb^*$ *age (Ma)* ±1σ	$^{207}Pb^*/^{206}Pb^*$ *age (Ma)* ±1σ	*Disc (%)*
40.1	96	96	1.03	0.124	1.964 ± 0.047	0.18214 ± 0.00149	1.966 ± 0.047	0.18118 ± 0.00156	2651 ± 52	2664 ± 14	0.5
40.2	286	263	0.95	0.102	2.186 ± 0.048	0.17290 ± 0.00095	2.188 ± 0.048	0.17209 ± 0.00102	2427 ± 45	2578 ± 10	5.9
41.1	60	25	0.43	0.181	1.958 ± 0.053	0.18316 ± 0.00193	1.962 ± 0.054	0.18175 ± 0.00213	2656 ± 60	2669 ± 19	0.5
42.1	227	116	0.53	0.047	2.031 ± 0.045	0.18289 ± 0.00099	2.032 ± 0.045	0.18252 ± 0.00103	2580 ± 47	2676 ± 9	3.6
43.1	166	165	1.03	0.063	1.993 ± 0.045	0.18219 ± 0.00113	1.995 ± 0.045	0.18169 ± 0.00115	2620 ± 49	2668 ± 11	1.8
44.1	54	63	1.19	0.072	1.945 ± 0.051	0.18476 ± 0.00205	1.946 ± 0.051	0.18421 ± 0.00212	2673 ± 57	2691 ± 19	0.7
45.1	20	7	0.36	0.164	2.011 ± 0.065	0.19483 ± 0.00349	2.015 ± 0.065	0.19357 ± 0.00350	2598 ± 69	2773 ± 30	6.3
46.1	96	80	0.86	0.111	1.978 ± 0.050	0.18339 ± 0.00152	1.980 ± 0.050	0.18253 ± 0.00161	2636 ± 54	2676 ± 15	1.5
47.1	146	88	0.62	0.126	1.999 ± 0.046	0.18405 ± 0.00123	2.001 ± 0.046	0.18307 ± 0.00133	2612 ± 49	2681 ± 12	2.6
48.1	299	332	1.15	0.096	2.243 ± 0.049	0.17582 ± 0.00087	2.245 ± 0.049	0.17507 ± 0.00097	2375 ± 44	2607 ± 9	8.9
49.1	147	77	0.54	–0.035	1.965 ± 0.045	0.18234 ± 0.00121	1.964 ± 0.045	0.18261 ± 0.00121	2653 ± 50	2677 ± 11	0.9
50.1	206	93	0.46	0.123	1.975 ± 0.044	0.18126 ± 0.00103	1.978 ± 0.044	0.18030 ± 0.00108	2638 ± 48	2656 ± 10	0.7
51.1	136	66	0.51	0.164	1.998 ± 0.046	0.18105 ± 0.00128	2.002 ± 0.046	0.17976 ± 0.00142	2612 ± 50	2651 ± 13	1.5
52.1	215	88	0.42	0.132	1.734 ± 0.039	0.22716 ± 0.00110	1.736 ± 0.039	0.22619 ± 0.00115	2933 ± 53	3025 ± 8	3.1
53.1	414	332	0.83	0.921	2.281 ± 0.050	0.18222 ± 0.00135	2.302 ± 0.050	0.17401 ± 0.00203	2325 ± 43	2597 ± 19	10.4
54.1	166	140	0.87	–0.013	1.982 ± 0.045	0.18102 ± 0.00119	1.981 ± 0.045	0.18113 ± 0.00122	2634 ± 49	2663 ± 11	1.1
55.1	123	68	0.58	0.295	1.954 ± 0.046	0.18450 ± 0.00138	1.960 ± 0.046	0.18220 ± 0.00158	2657 ± 51	2673 ± 14	0.6

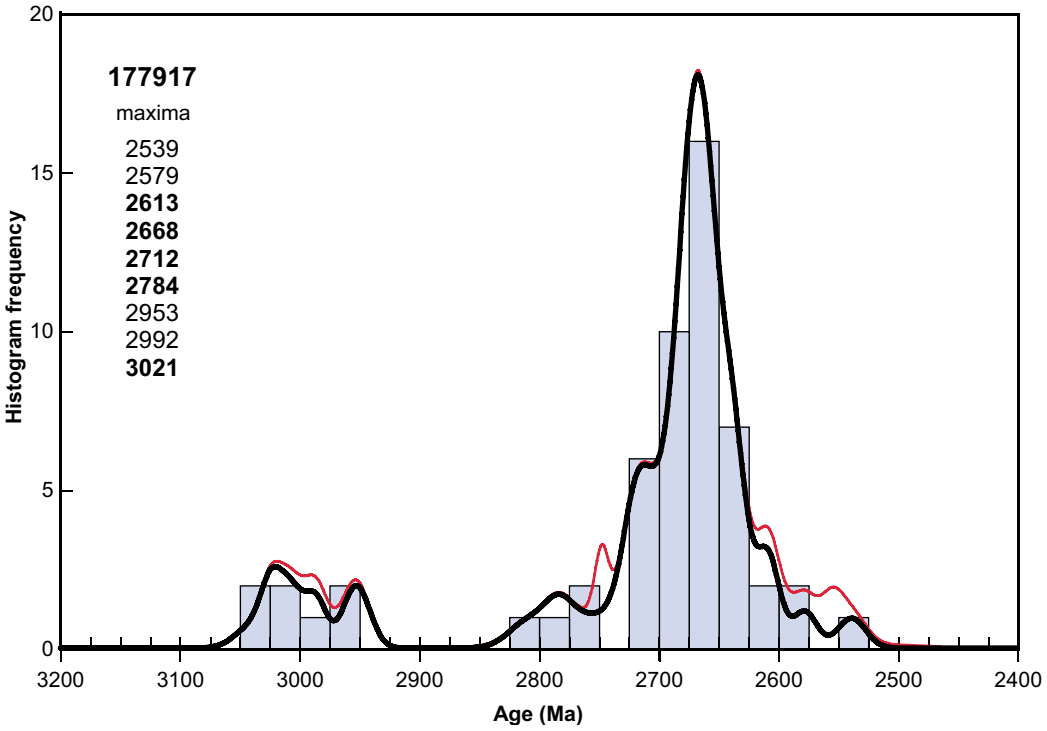

Figure 3. Probability density diagram for sample 177917: metamorphosed tuffaceous sandstone, Round Hill. Heavy curve, maxima values, and frequency histogram (bin width 25 Ma) include only data with discordance <10% and *f*204 <1% (54 analyses of 50 zircons). Light curve includes all data except discordant analysis 17.1 (60 analyses of 54 zircons)

and 55.1) with mostly very low common-Pb contents ($f204$ <0.2%), and $^{207}Pb^*/^{206}Pb^*$ ratios defining a single population, and indicating a weighted mean date of 2667 ± 5 Ma (MSWD = 0.72).

Group 3 comprises 18 concordant to slightly discordant analyses of 18 zircons (7.1, 8.1, 9.1, 10.1, 12.1, 15.1, 19.1, 22.1, 25.1, 26.2, 27.2, 29.1, 30.1, 31.2, 32.1, 34.1, 45.1, and 52.1) with mostly very low common-Pb contents ($f204$ <0.2%), and $^{207}Pb^*/^{206}Pb^*$ dates of 3038–2700 Ma.

Based on their common-Pb contents and discordance values, the 18 analyses in Group 1 are interpreted to have undergone at least one ancient episode of radiogenic-Pb loss, possibly during upper greenschist or lower amphibolite facies metamorphism. Consequently, the date of 2667 ± 5 Ma indicated by the 27 analyses in Group 2 is interpreted as the maximum age for deposition of the precursor tuffaceous sandstone. The remaining analyses have $^{207}Pb^*/^{206}Pb^*$ dates that define significant age components (based on three or more data-points) at c. 2712, c. 2784, and c. 3021 Ma, and minor components at c. 2953 and c. 2992 Ma. These are interpreted as the ages of zircon-bearing rocks in the detrital source region(s) of the precursor tuffaceous sandstone.

References

CASSIDY, K. F., CHAMPION, D. C., KRAPEŽ, B., BARLEY, M. E., BROWN, S. J. A., BLEWETT, R. S., GROENEWALD, P. B., and TYLER, I. M., 2006, A revised geological framework for the Yilgarn Craton, Western Australia: Western Australia Geological Survey, Record 2006/8, 8p.

JONES, S. A., in prep, Geology of the Erayinia 1:100 000 sheet: Western Australia Geological Survey, 1:100 000 Geological Series Explanatory Notes.

PAINTER, M. G. M., and GROENEWALD, P. B., 2001, Geology of the Mount Belches 1:100 000 sheet: Western Australia Geological Survey, 1:100 000 Geological Series Explanatory Notes, 38p.

STACEY, J. S., and KRAMERS, J. D., 1975, Approximation of terrestrial lead isotope evolution by a two-stage model: Earth and Planetary Science Letters, v. 26, p. 207–221.

Recommended reference for this publication

BODORKOS, S., LOVE, G. J., NELSON, D. R., and WINGATE, M. T. D., 2006, 177917: metamorphosed tuffaceous sandstone, Round Hill; Geochronology dataset 624, *in* Compilation of geochronology data, June 2006 update: Western Australia Geological Survey.

Data obtained: 25 October 2004
Data released: 30 June 2006